Fatigue analysis of the main frame of over head transportation vehicles using flexible multibody dynamics[†]

Ji Won Yoon[1], Sung Pil Jung[1], Tae Won Park[2,*] and Joong Kyung Park[3]

[1]Graduate School of Mechanical Engineering, Ajou University, San5 Woncheon-dong, Yeongtong-gu, Suwon 443-749, Korea
[2]Department of Mechanical Engineering, Ajou University, San5 Woncheon-dong, Yeongtong-gu, Suwon 443-749, Korea
[3]Samsung Electronics Co. Ltd, 416, Maetan-3 dong, Yeongtong-gu, Suwon, 43-370, Korea

---

Abstract

The industrial over head transportation vehicle is a guided railway vehicle that is attached overhead and transports cargo, hoisting it up and down from the factory ceiling. The vehicle is widely used in many industries, such as automobile and liquid crystal display (LCD), because it can carry freight very safely and quickly to destinations. This kind of freight transportation usually operates for several months to a few years, carrying large amounts of products. Accidently, the vehicle often fails during operation because of a part's plastic deformation from large loads. Furthermore, periodic dynamic loads cause fatigue accumulation, which leads to OHT failure. This failure is directly connected to significant economic loss during mass production processes. Therefore, the prediction of fatigue life for the important parts becomes an important task. In this study, the fatigue life of an OHT main frame was calculated and predicted by using a flexible multibody dynamic model. The development of a flexible multibody dynamic model and the procedure of fatigue life prediction were presented. To predict the fatigue lives of parts of interest, the prediction procedure required three kinds of data: Dynamic stress time history from a dynamic analysis, material properties of the parts, and stress-life curves of the parts. Using a finite element model and a multibody model, a flexible multibody model was developed. To ensure the reliability of the model, displacement and strain measurement tests were conducted. After verification of the reliability, the fatigue life of the main frame was predicted.

Keywords: Multibody dynamics; Dynamic analysis; Over head transportation; Modal stress recovery (MSR); Fatigue analysis

---

1. Introduction

The over head transportation (OHT) vehicle is in greater demand than previously because it has advantages in carrying many products simultaneously and efficiently using the upper level of factory space, which is usually unused. However, there is also greater demand for faster speed and larger capacity to increase productivity, but such a demand often leads to higher risks of fatigue failure, which is a serious problem. The OHT vehicle can operate for several months to a few years, carrying large amounts of products. During the operation period, it can fail due to the plastic deformation of a part and crack arising from large amounts of dynamic load. Additionally, a periodic, repeated dynamic load causes fatigue damage accumulation and leads to failure. Naturally, the failure is linked with serious risks, specifically the safety of the operator, who works underneath the vehicle. Therefore, to prevent vehicle risks and ensure the safety of the vehicle and its operator, a

fatigue life evaluation of the vehicle in the design stage is crucial.

The purpose of this research was to predict the fatigue life of the vehicle main frame. To predict the fatigue life of a vehicle part of interest, a dynamic analysis model, which includes the rigid and the flexible body, was developed. Dynamic analysis is useful for evaluating the dynamic load applied to the part of interest. Also, various behaviors of the part of interest can be predicted according to the operation scenario, such as operation on a straight railway and operation on a curved railway while it is accelerating, decelerating, loading, and unloading cargo. The reliability of the dynamic model was investigated and validated by a test operation and a strain gauge test of interest points. A reliable multibody dynamic model is helpful not only to assess the loading condition but also to identify the dynamic behavior of the vehicle.

2. Procedures for fatigue life analysis

To extract the loading information for fatigue analysis, a reliable multibody dynamic model with proper boundary conditions is necessary. With proper modeling, dynamic stress time
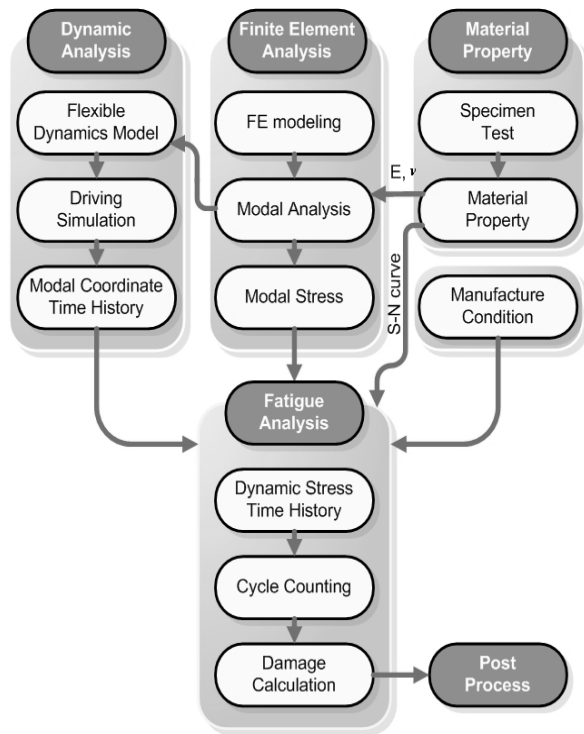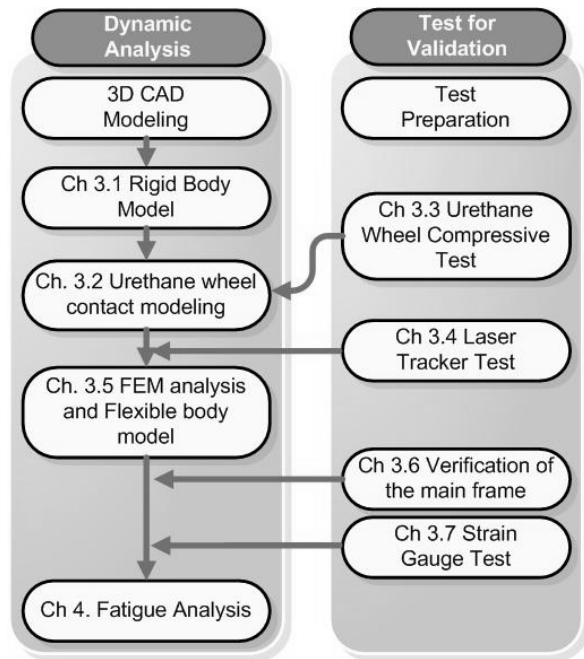

Fig. 1. Fatigue analysis procedure.

Fig. 2. Dynamic modeling and required test.

history (DSTH) of the part of interest can be extracted. Since boundary conditions for a running vehicle are difficult to obtain, a finite element (FE) model should be incorporated into the dynamic model based on the modal analysis information of the parts of interest. This process can easily demonstrate the flexibility effects of the multibody model. Therefore, modal analysis information is acquired and superposed to evaluate
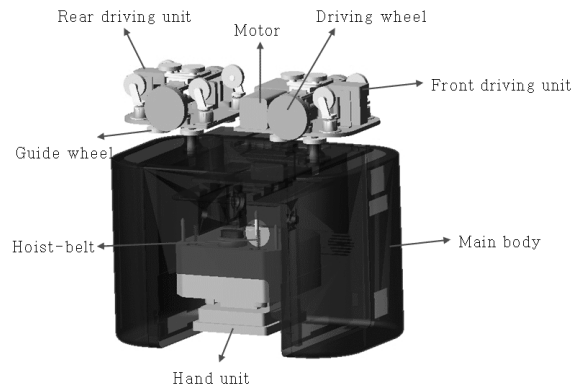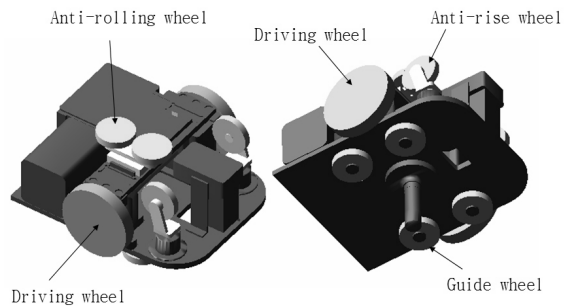

Fig. 3. Dynamic modeling.

Fig. 4. Details of the front driving unit.

the deflections of parts of interest. Once the dynamic model is verified, the material properties can be applied and fatigue analyzed, as shown in Fig. 1 [1].

It is essential to perform a multibody dynamic analysis, which calculates a more accurate modal response considering the inertia effect [2].

In this study, the main frame of an OHT vehicle was selected as a subject for investigation because it has to be the most secure to give proper structural support for all the other bodies. It is connected by six joints and interacts with other parts during operation. If the part breaks during operation, all the other parts need to be overhauled for repair and replacement.

Since the fatigue analysis needed to be initially carried out, the rigid and flexible body dynamic analyses were conducted, followed by the relevant verification of the model, as shown in Fig. 2. Fig. 2 shows the required test and chapter indices for contents in Chap. 3.

3. Dynamic analysis

3.1 Rigid body model

When creating a dynamic model, the three dynamic characteristics should be considered, namely, the rolling contact between a driving wheel and the rail, the rolling contact between a guide wheel and the rail, and the rolling motion of the main body. To build a realistic model, the following procedures, described in Fig. 2, were performed [2].
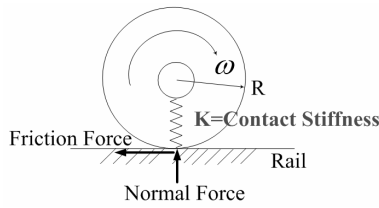
Fig. 5. Dynamic modeling of the wheel.

Fig. 3 shows the overall structure of the OHT vehicle, which is composed of the main body, driving unit, wheels, hoist unit, and hand unit. The front and rear driving units have 10 and 12 wheels, respectively. The front driving unit, shown in Fig. 4, has two driving wheels, four guide wheels under the main body, two antirolling wheels for the curved rails, and two antirise wheels but, otherwise, four antirise wheels for the rear driving unit. Wheels are urethane wheels of outer urethane rubber and inner aluminum frame. The electric motor is located in the front driving unit. A urethane-made hoist belt is attached to the inside of the main body and is controlled by the hoist unit, which changes the length of the hoist belt to change the elevation of the hand unit. Kinematically, the multibody dynamic model has 32 bodies, 22 revolute joints, and six fixed joints with 30 degrees of freedom.

3.2 General information about urethane wheel contact modeling

Four main wheels in the system support the total vehicle weight and provide sustainable contact to drive the vehicle back and forth. The electric motor only drives the front driving unit. The contact force between the wheels and rails is modeled by a solid-solid contact element in ADAMS/View.

When creating the rolling contact dynamic model, complicated wheel/rail contact was not assumed because the main concern was the vertical movement of the system. The rolling contact of this system is somewhat different from that of a wheel/rail contact. Therefore, the effects of conicity, slip, and flange contact were not considered [3], and so the rolling contact was simplified to a Hertzian contact. The effective coefficients when evaluating a contact model are stiffness, exponent n, damping, and friction. Among these, the stiffness and the exponent coefficient were obtained from a compressive test, as shown in Chap. 3.3.

3.3 Urethane wheel compressive test

To define the contact parameters of the wheels, a compressive test was performed. Contact stiffness and contact exponent are the key parameters in the evaluation of contact parameters. The simplified Hertzian contact equation is shown in Eq. (1) and Fig. 5.

$$F_{normal} = K\delta^n + D\dot{\delta}, \qquad (1)$$

where K is the contact stiffness, D is the contact damping,

Table 1. Contact parameters.

Wheel type	Driving wheel	Guide wheel
Contact stiffness	1450	1700
Contact exponent	1.3	1.4
Static friction coefficient	0.8	
Dynamic friction coefficient	0.6	

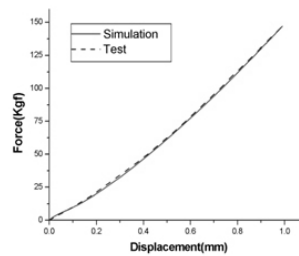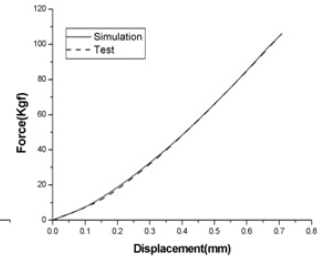
Fig. 6. Driving wheel test.   Fig. 7. Guide wheel test.
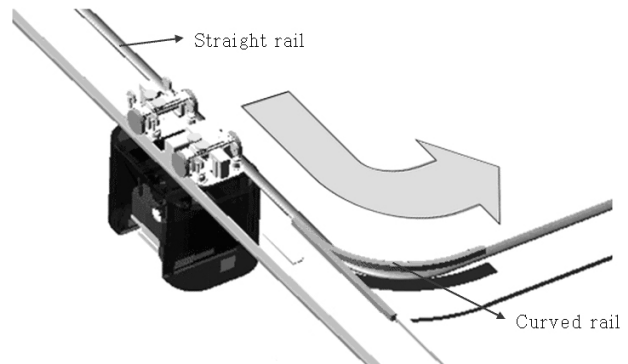

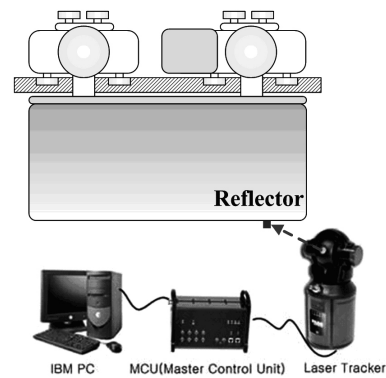
Fig. 8. An operation scenario.

Fig. 9. A schematic diagram of a laser tracker test.

and n is the contact exponent indicating the nonlinear characteristics of the normal force. The data given in Table 1 were extracted from the urethane wheel compressive test. By comparing the displacement versus force data, the parameters for the simulation model were chosen by trial and error, as shown in Table 1. To validate these parameters, a compressive test was done. The Hertzian simulation contact model is well matched with the test data, as shown Figs. 6 and 7.

3.4 Verification of rigid body model by laser tracker test

To evaluate the dynamic behaviors of the target system, a driving test is required. The test results were compared with the results obtained from the dynamic model to verify the reliability of the dynamic model. Hence, three-dimensional (3D) displacement measurement tests were done by using a laser tracker system. A laser tracker system is a measurement instrument possessing high resolution and precision. It measures the distance from the tracker to the origin of the test plane and is commonly used for industrial purposes. With the test, the dynamic behavior of the vehicle can be understood. Fig. 8 shows operation test scenarios. Fig. 9 shows a schematic installation diagram of the laser tracker 3D displacement test. A reflector was attached under the center-front section of the main body. Three-dimensional displacement tests were executed for two cases.

The vehicle ran along a curved rail. In total, ten tests were screened and carried out. In Fig. 10, the X-Y plane trajectory test result is shown and compared with the simulation data.

In this case, the vehicle swung out in the curve, as shown in Fig. 10, due to the lateral acceleration when the vehicle ran along a curved rail. Fig. 11 shows the vertical displacement.
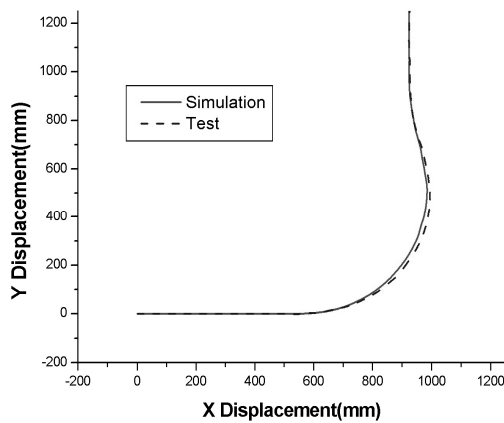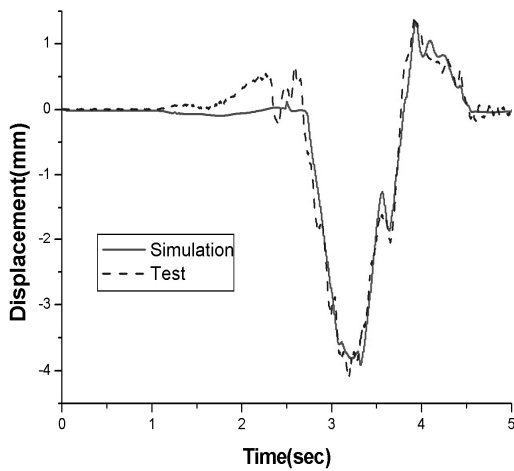
After 2 s from the start of movement, the vehicle approached the curve. The first peak that occurred at about 2.3 s in Fig. 11 was caused by shock the vehicle experienced upon entering the curved rail. The initial data error was thought to be caused by an installment problem of the rail, such as the welded rail junction, upon inspection by a field engineer. After entering the curved rail, a downward displacement occurred because of the roll motion and the load transfer from the driving wheel to the antiroll wheel, and finally, the main body stabilized after the vehicle re-entered another straight rail. The test and simulation, thus, verified the reliability of the dynamic model.

In Figs. 10 and 11, the test results and simulation are well matched. However, both results can vary by how the circum-

Table 2. Properties of the FE model.

Type of material	Aluminum 6061-T6
Young's modulus	68.9 GPa
Poisson's ratio	0.33
Density	2.7 g/cm3
Number of nodes	23292
Number of elements	16790
Element type	Hexahedron

Fig. 10. Comparison of XY trajectories.
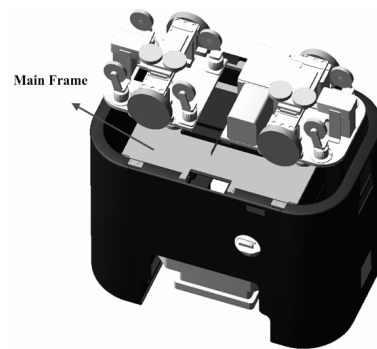

Fig. 12. Location of the main frame.

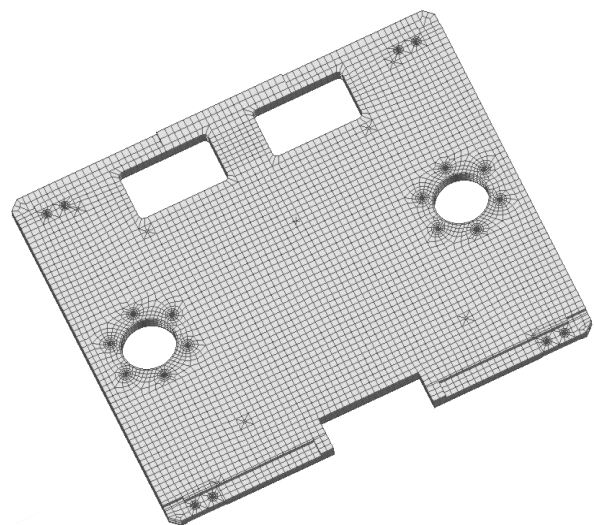Fig. 11. Comparison of vertical displacements.

Fig. 13. Finite element model of the main frame.

stances of the experiment are managed and how the model is simulated.

3.5 FEM analysis and flexible body model

The DSTH is a critical piece of data necessary for achieving the most reliability of the vehicle. In addition, a strain gauge test and flexible body dynamic simulations should be performed to verify the reliability of the flexible body model. Among the many bodies in the vehicle, the main frame is the most important body that should be analyzed by fatigue life analysis. Therefore, the FE model for the main frame was developed and inserted into the dynamic model shown in Fig. 3. The FE model of the main frame was configured as shown in Fig. 12 by MSC. Nastran/Patran. The material properties of the FE model were provided by the manufacturer, as given in Table 2.

Table 3. Comparison of test and FE analysis results.

Mode	Test (Hz)	FE Analysis (Hz)	Error (%)	Shape
1st	143	143.74	0.5	1st torsion
2nd	199	199.45	0.2	1st bending
3rd	296	297.27	0.4	2nd bending
4th	373	375.25	0.6	Torsion+Bending

Fig. 14. Test measurement points.

<1st mode shape>   <2nd mode shape>

<3rd mode shape>   <4th mode shape>

Fig. 15. Mode shapes from test results.

3.6 Verification of the main frame by a modal test

To verify the integrity of the FE model, a modal test was performed to examine the natural frequency of the main frame. As shown in Fig. 13, an accelerometer was attached to the main frame, and 25 points of excitation were selected to be hammered for the measurement. Table 3 gives the modal test results and the comparison of these results with FE analysis results.

Figs. 15 and 16 show the mode shapes from the test and the simulation results, respectively. As shown in Table 3, the error between the test and simulation was less than 1%, demonstrating the FE model is reliable enough to be used for flexible dynamic analysis.

3.7 Verification of the flexible body model by a strain gauge test

Using the flexible multibody dynamic model, deflection, stress, and strain of the FE model can be extracted. To identify the DSTH of the main frame, a rosette and strain gauge from Tokyo Sokki Kenkyujo Co. were used and attached. The vehicle running at two different velocities, 0.5 and 0.8m/s, respectively, in the curved rail was profiled. As shown in Fig. 16, three-axis 45° rosettes were installed on the main frame. The number in Fig. 17 is the input channel number of the instru-
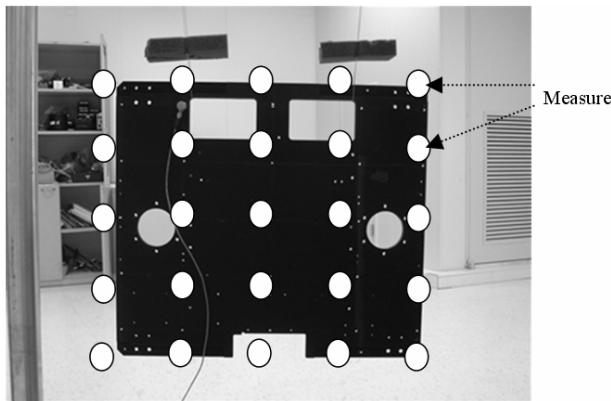

<1st mode shape>   <2nd mode shape>
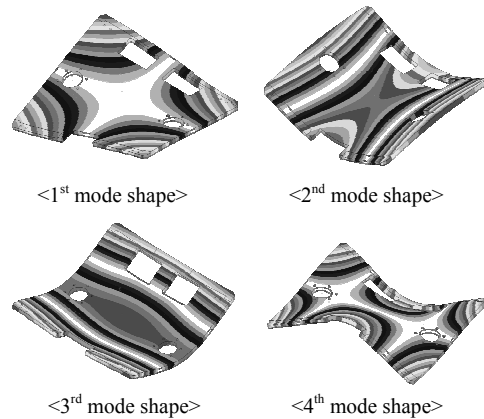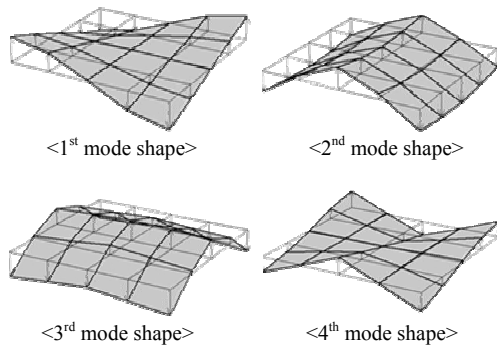
<3rd mode shape>   <4th mode shape>

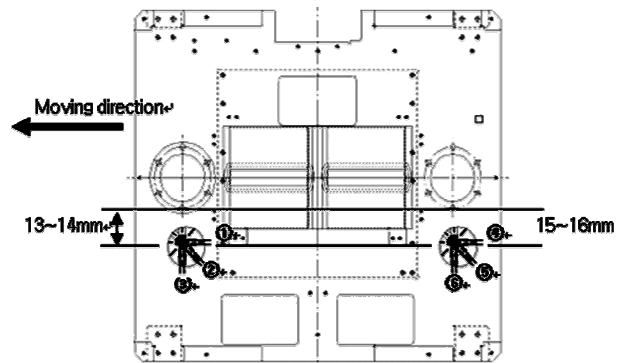Fig. 16. Mode shapes from analysis results.

Fig. 17. Position of the attaching rosettes for the main frame.

ments. Ten experiments per velocity were performed, and they gave almost the same results. The conditions applied for the flexible multibody simulation model were the same as those for the test.

The final test results are shown in Figs. 18 and 19. The strain did not change greatly with the changes in velocity. However, it was found that the greater the velocity, the greater the fluctuation of the strain value. At all velocities, the data from the front and rear strain gauge have opposite signs, showing the main frame was suffering from the torsional motion. DSTH results were obtained from the same spots where the strain gauges were attached. Among the input channels of the rosettes, channels 1, 3, 4, and 6, which are related to the vehicle-fixed longitudinal (X) and lateral (Y) coordinates, were used for data comparison.

The simulation and test results show similar behavior, as shown in Figs. 18 and 19. The strain increased slightly when

the velocity increased, demonstrating the reliability of the flexible multibody model.

The number of elements was doubled and quadrupled to identify the influence of the number of elements in the FE model on the results. All other design parameters were fixed and modeled as in the original model, except for the number of elements. Table 4 shows the number of elements and nodes of each FE model.

In Fig. 20, although the number of elements was increased, the results are identical to the results from the original model, suggesting the current FE model is reliable enough and the number of the elements is also sufficient for application of the FE model to flexible dynamic analysis.

4. Fatigue life analysis

4.1 Fatigue life prediction

Using the data from the DSTH information of the modal stress recovery (MSR) method and stress-life curve, the fatigue life of the main frame was calculated. The MSR method superposes the modal information to calculate the deformation of the part of interest and, finally, the modal dynamic stress [4-6].

Although these procedures can be performed by a commercial FE analysis program, a dynamic analysis program was used because it can consider the inertia effect of the parts easily. Specifically, the main frame is constrained by six joints and interacts with other bodies. In this sense, it is more efficient to calculate the modal response using multibody dynam-
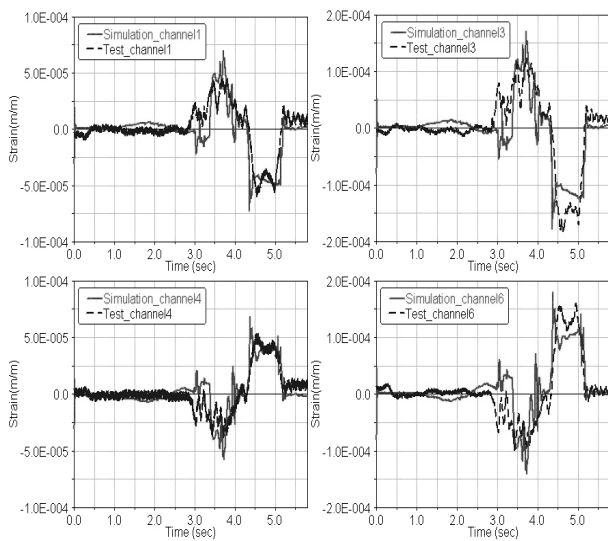

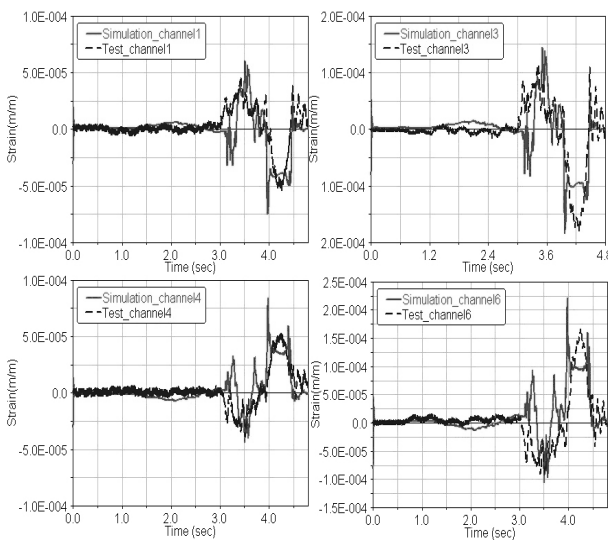Fig. 18. Comparison of analysis and test results for 0.5 m/s.

Fig. 19. Comparison of analysis and test results for 0.8 m/s.

Table 4. Element properties of each FE model.

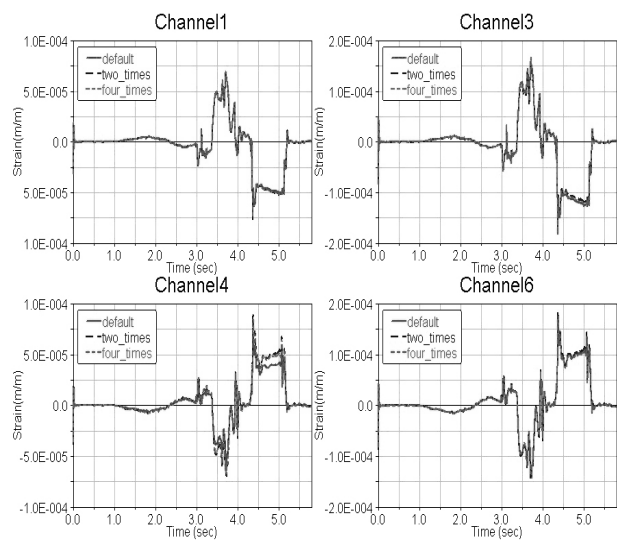| Main frame	Default	2 times	4 times
Number of nodes	23,292	40,981	86,740
Number of elements	16,790	31,066	66,738

Fig. 20. Comparison of results by increasing the element number.

ics. MSC.ADAMS offers durability modules for flexible body dynamic analysis, which provides the modal response and modal stress time history [7]. Users do not have to manually superpose the modal data to calculate DSTH.

In Fig. 21, the first two processes were processed by MSC.Nastran/Patran, and the third process was performed by the MSC.ADAMS/Flex module to create the modal neutral file (MNF) [7]. The model for the fourth procedure was simulated by ADAMS and analyzed by the Durability module to produce the input file for the commercial fatigue analysis program, FE-Fatigue. For the last part, MSC.FE-Fatigue was used to calculate the fatigue life.

The FE model for the main frame is shown in Fig. 13. The stress-life curve and its material properties were selected from the table of aluminum 6061 [8]. Mode shapes were categorized in the following manner. Generally, there are two types of modes: normal mode and static mode. Static mode is further divided into attachment mode and constraint mode. Attachment mode is defined as the static deflection of a component that results when a unit force is exerted on one coordinate and no force is exerted on the remaining coordinates [9]. A constraint mode is defined by statically imposing a unit displacement on one physical coordinate and zero displacement on the remaining coordinates. Generally, MSC.ADAMS recommends the use of the normal mode and constraint mode. Using the commercial FE analysis program, MSC.Nastran/ Patran, 20 normal modes and 36 constraint modes were calculated and transformed to MNF. In this process, component mode synthesis (CMS) included the orthonormalization proc-

ess. Finally, 56 pieces of orthonormalized modal information were included in MNF. After CMS, the modal analysis results for the main frame were summarized, as shown in Table 4. The most influential modes are depicted in Fig. 22. Mode shapes from Fig. 22, the seventh to tenth mode shapes, became the actual first to fourth modes when the rigid modes from Table 5 were excluded.

Modal analysis shows the main frame has mode frequencies ranging from 157 to 34665 Hz, and all 56 modes were selected for simulating the flexibility effects. The target life was set as Eq. (2). According to the installment plan for the vehicle, the vehicle passes the straight and curved rail 1,344 times a day. If the vehicle operates for 5 years with 70% usage rate, the total operating time is calculated as follows for a safety factor (SF) of 3. SF is generally the value of strength divided by the stress level. When designing mechanical elements, the static SF is set to be the same as the dynamic SF to obtain a reliable design [9]. If the SF value is set high enough, the machine probably will not break during operation; however, this will not be economically profitable. If one sets the SF value to a margin minimum value, the production cost can be reduced, but critical safety and durability problems can arise. Although there is no standard SF value, there are some recommendations, as shown in Eq. (3) [10]. In our study, an SF value of 3 was chosen. Therefore, the target life was set by

$$
\begin{aligned}
Target\ Life &= 1344\,times\,a\,day \times 365\,days \\
&\quad \times 5\,years \times 70\% \times 3\,(safety\,factor), \\
&= 5,150,880\,Repeats
\end{aligned} \tag{2}
$$

$$
\begin{aligned}
&Dynamic\ SF \geq 1.25\ for\ symmetrical\ stress \\
&Static\ SF\quad \geq 2.50\ for\ ultimate\ strength\quad, \\
&Static\ SF\quad > 2.50\frac{S_y}{S_u}\ for\ yield\ strength
\end{aligned} \tag{3}
$$

Table 5. Results of trolley modal analysis (unit: hertz).

Mode	Frequency	Remark
1-6	0	Rigid mode
7	157	1st torsion
8	203	1st bending
9	349	2nd bending
10	433	Torsion +bending

Fig. 21. General analysis procedures for extracting DSTH.
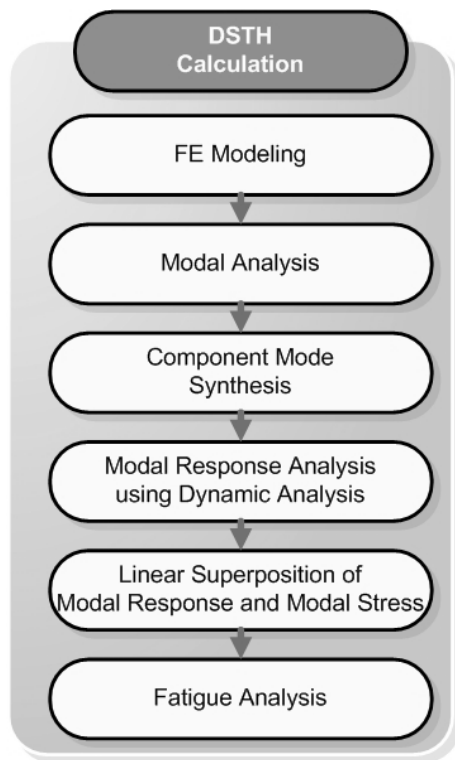

<7st mode shape> <8st mode shape>
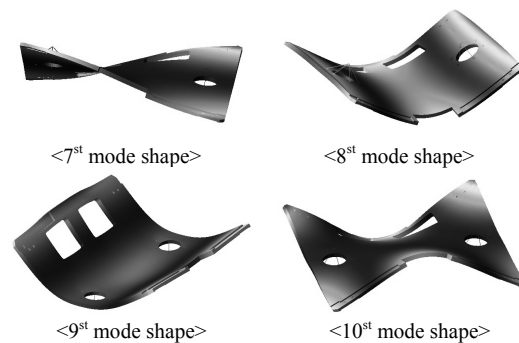
<9st mode shape> <10st mode shape>

Fig. 22. The mode shapes of the main frame.

where S_y and S_u are the yield strength and ultimate strength, respectively.

The simulation scenario was planned as follows. To meet the demands for higher productivity after commercialization, the vehicle, which currently operates at 0.5 m/s on a curved rail, will run at 0.8 m/s, the target speed. For this reason, fatigue life was predicted for these two velocities. Modal response results for the OHT vehicle are shown in Figs. 23-26. The figures show the strain data according to the mode. According to the result, the seventh to tenth modes contribute the most in modal response. This means these modes contribute the most proportion of deflection, and accordingly, the stress of the main frame highly depends upon them. Especially the first bending mode, the eighth mode, contributes most to the modal response. The plate suffers bending motion frequently by the pitch motion when the vehicle accelerates, decelerates, and runs on the curved rail. By Miner's linear damage rule and rain flow cycle counting method, fatigue life can be predicted.
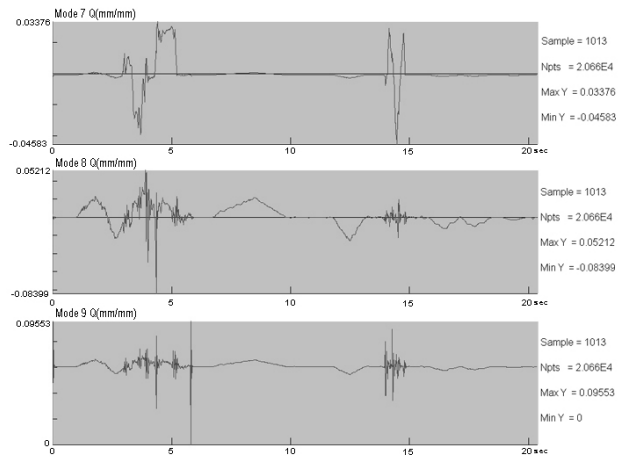

Fig. 25. Modal responses of the main frame at the target velocity (0.8 m/s).
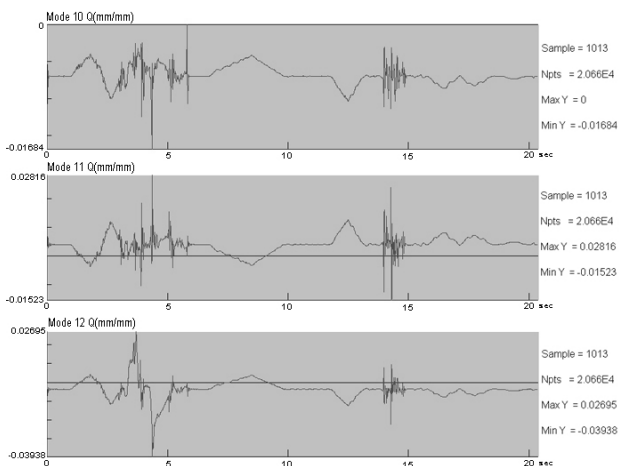

Fig. 23. Modal responses of the main frame for the present velocity (0.5 m/s).

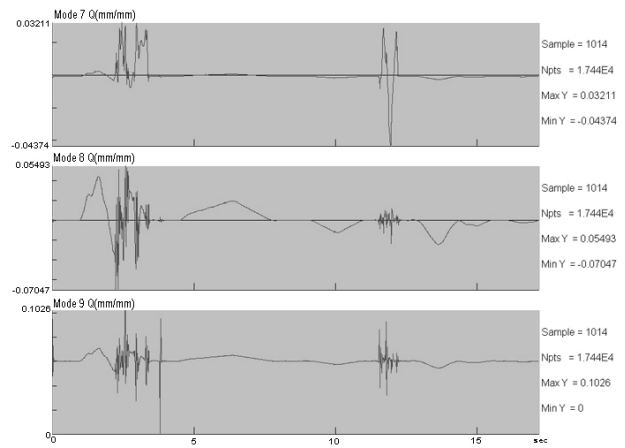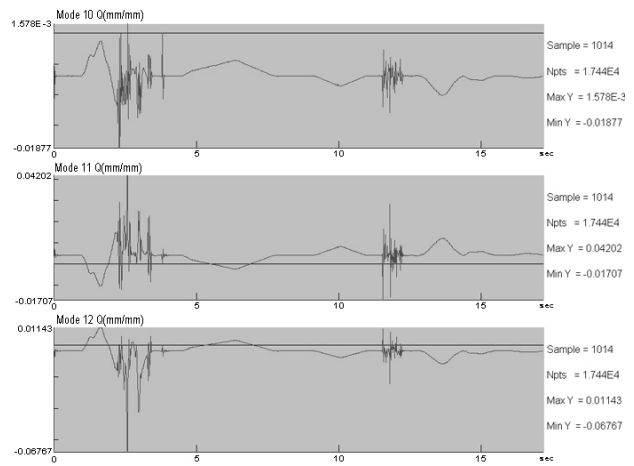Fig. 26. Modal responses of the main frame at the target velocity (0.8 m/s).

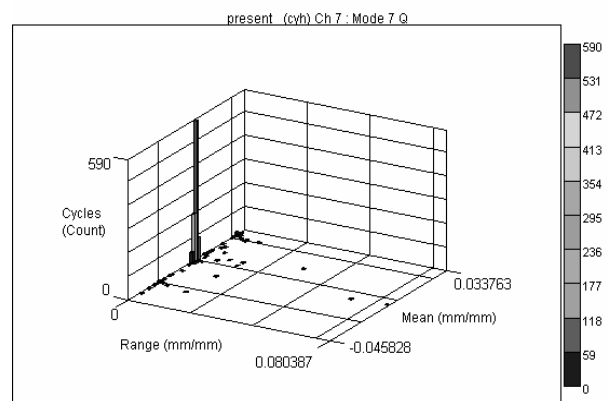Fig. 24. Modal responses of the main frame at the present velocity (0.5 m/s).

Fig. 27. Cycle counting of the main frame seventh modal response at the present velocity.
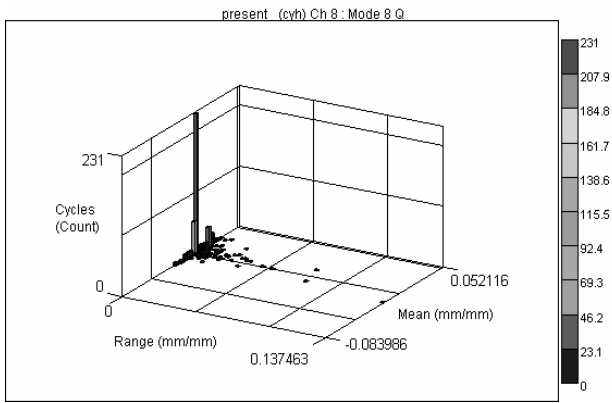
Fig. 28. Cycle counting of the main frame eighth modal response at the present velocity.
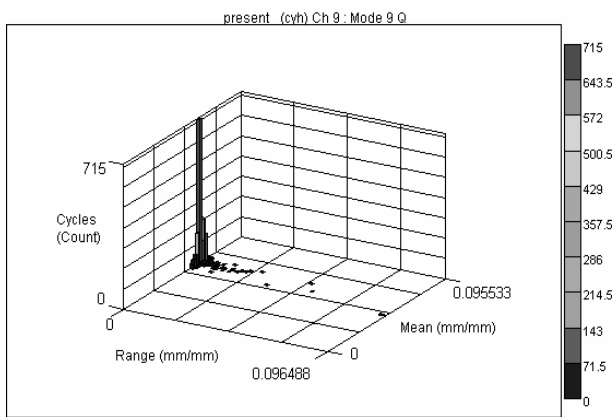

Fig. 29. Cycle counting of the main frame ninth modal response at the present velocity.
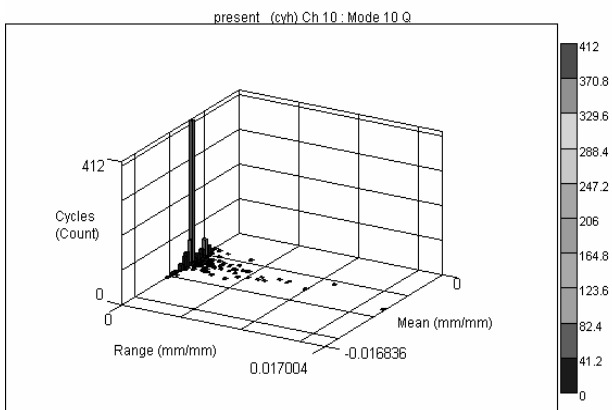

Fig. 30. Cycle counting of the main frame tenth modal response at the present velocity.

Each cycle counting results are depicted in Figs. 27-30. The fatigue life for each velocity calculated by FE-Fatigue is shown in Table 6, and the damage distribution for each velocity is depicted in Figs. 31 and 32. As shown in Figs. 31 and 32,

Table 6. Results of trolley fatigue analysis (unit: repeats).

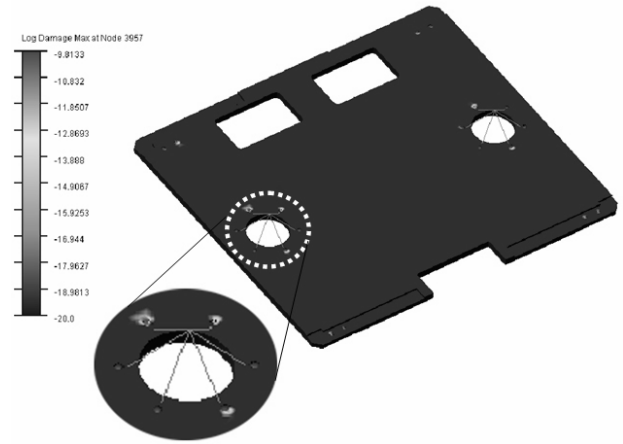| Mean stress	Goodman	Gerber	No mean
Present velocity	6.51E9	2.54E10	1.81E10
Target velocity	8.91E7	1.08E9	4.54E8

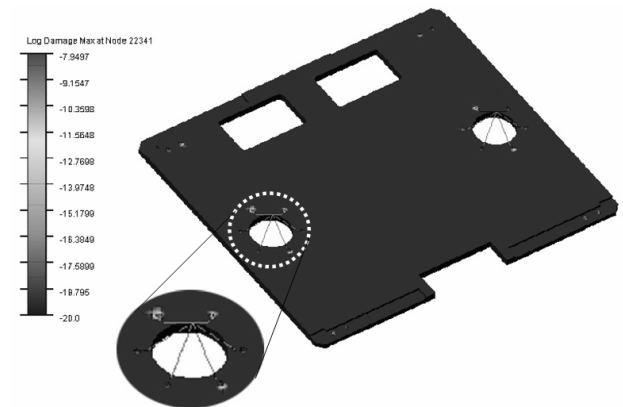Fig. 31. Log damage contour of the main frame for the present velocity.

Fig. 32. Log damage contour of the main frame for the target velocity.

the damage distribution for each velocity shows the same area near the bolt hole on the main frame is crucial. The maximum damage value at the target velocity is greater than that at the current velocity. Furthermore, in the case of the main frame, the most damaged area is expected to be under periodical compressive mean stress. Therefore, the mean stress effect should be considered when estimating the fatigue life.

To be conservative, the Goodman line would be more appropriate in judging the fatigue life.

The fatigue life of the main frame is calculated as in Table 5. In Goodman's results from Table 5, the final results, 6.52E9 for the present velocity and 8.91E7 for the target velocity, are much larger than the predefined target life, 5.2M repeats. Therefore, the current design of the main frame has infinite fatigue life and is safe enough to satisfy the current operation.

5. Conclusion

First, a reliable dynamic model is required to predict a proper fatigue life. In this research, both rigid and flexible body dynamic models were developed and verified based on the design specification and component test data of the OHT vehicle. The verified model was used to predict the dynamic behavior of the vehicle on various railways operated according to a schedule, such as acceleration and deceleration and loading and unloading of freights. The main aluminum frame, which is the part of most interest, was translated into an FE model, and it was also verified by modal tests. According to the proposed procedures for fatigue life analysis, three kinds of data, DSTH, modal stress, and S-N curve, were synthesized and analyzed to predict the fatigue life. The fatigue life of the main frame was longer than the desired target life. The method summarized in this paper can be used to reduce the time and cost for designing other vehicles to be used in different environments and conditions.

References

[1] Julie A. Bannantine, Jess J. Comer and James L. Handrock, Fundamentals of metal fatigue analysis, Prentice Hall, (1989).

[2] T. W. Park, J. H. Seo, K. J. Jun, H. J. Yim, H. Kim and J. K Park, A study on the fatigue life prediction of the OHT vehicle stuructures using the modal stress recovery method, Il-ho jung, DETC2005-84319, Proceedings of IDETC/CIE (2005).

[3] J. J. Kalker, Three-dimensional elastic bodies in rolling contact, Kluwer Academic Publishers, (1990).

[4] T. R. Jeon, H. Shin and J. S. Choi, Fatigue analysis of air compressor bracket by using modal superposition method, Vol. I, *The Korean Society of Automotive Engineers* (2006) 668-672.

[5] H. J. Lee, J. H. Won, S. J. Son, S. Heo and J. H. Choe, Fatigue Life Prediction Algorithm and Durability Analysis Programming of Vehicle Components, Vol. II, *The Korean Society of Automotive Engineers* (2006) 1345-1352.

[6] I. H. Jung, T. W. Park, C. S. Kim, D. H. Cho and J. K. Park, A Study on Dynamic Analysis and Fatigue Life of the Belt in the OHT Vehicle, *The Korean Society of Mechanical Engineers* 29 (8) (2005) 1085-1092.

[7] MSC. ADAMS reference manual

[8] http://www.matweb.com

[9] Roy R. Craig, Structural Dynamics, Jr. John Wiley & Sons, (1983).

[10] S.-M. Yang, H.-Y. Kang and K.-H. Kim, An estimation reliability of machine elements subjected to fluctuating load considering static and dynamic allowable safety factors, *The Korean Society of Automotive Engineers* 15 (4) *(1998)* 51-57.

Ji Won Yoon Ph.D. in Mechanical Engineering from Ajou University, Suwon, Korea. Academic interests in multibody dynamics and flexible bodies. Currently, he is in a postdoctoral course and a research engineer in Research Center for Automotive Parts Technology, Ajou University.

Tae Won Park Ph.D. in Mechanical Engineering from University of Iowa, USA. Academic interests in multibody dynamics, flexible bodies, control and fatigue. Currently, he is a professor in Ajou University, working actively in various fields, such as railway vehicle, brake system and fatigue estimation.